Pharmaceutical Research, Vol. 23, No. 7, July 2006 (© 2006)
DOI: 10.1007/s11095-006-0254-1

Research Paper

Dealing with Time-Dependent Pharmacokinetics during the Early Clinical Development of a New Leukotriene B_4 Synthesis Inhibitor

Iñaki F. Trocóniz,[1] Ilonka Zsolt,[2,3] María J. Garrido,[1] Marta Valle,[2] Rosa M. Antonijoan,[2] and Manel J. Barbanoj[2,4]

Received October 4, 2005; accepted February 16, 2006

Purpose. The aim of this study was to explore the possibility of achieving a practical dosing regimen for 2,4,6-triiodophenol (AM-24), a new leukotriene B_4 (LTB_4) synthesis inhibitor. First, a model capable of dealing with the nonlinearity in its pharmacokinetic profile was built, and then it was combined with a pharmacodynamic model previously established with data from earlier phase I trials.
Methods. One week after the first 240-, 350-, or 500-mg oral dose of AM-24, six additional doses were given to 24 healthy volunteers once daily. A total of 33 blood samples were obtained from each individual. Different models, including enzyme turnover models, were fitted to the data by using the software NONMEM.
Results. Drug absorption was modeled with a first-order process. Drug disposition was described with a one-compartment model, and elimination with an (auto)inhibited and a noninhibited clearance. AM-24 inhibited the enzyme production rate to a maximum of 98%. Relative bioavailability was independent of the decrease in the amount of enzyme. The estimate of the enzyme turnover half-life was 8.5 h.
Conclusions. Simulations have shown that steady-state conditions eliciting 90% of maximal LTB_4 synthesis inhibition can be reached after 3 weeks during an oral treatment with AM-24 administered at the dosage of 500 mg once daily.

KEY WORDS: metabolism autoinhibition; NONMEM; population pharmacokinetics.

INTRODUCTION

Many factors can lead to a discontinuation in the development of a new drug. Whereas approximately 50% of the failures are caused by lack of efficacy, adverse effects, or animal toxicity, almost 40% of failures are caused by poor pharmacokinetic characteristics (1). Slow absorption rate, low bioavailability, poor tissue penetration, nonlinear behavior, presence of toxic metabolites, or high variability are examples of limited pharmacokinetic properties (2), and to find out if they can be overcome with the currently available tools is a challenge. In addition to pharmaceutical technology, which is used routinely to improve absorption and distribution properties (3,4), data modeling helps in the case of nonlinear kinetics to identify the cause(s) of nonlinear kinetics by discriminating between competing hypotheses, the onset and offset, and the clinical impact of the nonlinearity (5,6).

2,4,6-Triiodophenol (AM-24) is a potent leukotriene B_4 (LTB_4) synthesis inhibitor that is currently under clinical development. The exact mechanism of action of AM-24 is not completely understood, but it is known that the inhibition of the enzyme 5-lipooxygenase is involved (data on file from Industrial Farmacéutica Catabria, S.A., Spain). Results obtained from the first phase I clinical trial, in which a single dose was administered orally to healthy volunteers, showed that AM-24 had good safety and tolerability profiles (studied doses: 6, 30, 60, 120, 240, 350, 500, 700, and 1200 mg). AM-24 showed linear pharmacokinetics in the dose range 6 to 700 mg. A nondose proportional increase in the area under the drug plasma concentration *vs.* time curve (AUC) was found for the 900- and 1200-mg doses, a finding that suggests saturable enzymatic kinetics. Drug absorption and disposition could be described with a first-order rate of absorption model and a one-compartment disposition model, respectively. A direct and nonlinear (E_{MAX} type) relationship between plasma concentrations and LTB_4 synthesis inhibition with an IC_{50} value (the level of drug in plasma eliciting half of maximal LTB_4 synthesis inhibition) of 16.6 μg/mL was also found (data on file from Industrial Farmacéutica Catabria, S.A., Spain). Hysteresis was not present in the plot of the percentage of LTB_4 reduction *vs.* drug concentrations in plasma. Similar results

[1] Departmento de Farmacia y Tecnología Farmacéutica, Facultad de Farmacia, Universidad de Navarra, Pamplona, Spain.
[2] Centre d'Investigació de Medicaments, Institut de Recerca de l'HSCSP, Servei de Farmacologia Clínica, Hospital de la Santa Creu i Sant Pau, Departament de Farmacologia i Terapèutica de la Universitat Autònoma de Barcelona, Av Sant Antoni M Claret 167, 08025 Barcelona, Spain.
[3] Present Address: Sanofi-Aventis, S.A.U., Barcelona, Spain.
[4] To whom correspondence should be addressed. (e-mail: mbarbanoj@santpau.es)

0724-8741/06/0700-1533/0 © 2006 Springer Science + Business Media, Inc.

Table I. Individual Demographic Characteristics

	Mean	Range
Age (years)	26.12	20–32
Weight (kg)	74.30	54.1–92.0
Height (cm)	178.08	157–194
Body mass index[a] (kg/m^2)	23.83	20–26

[a] Computed as the ratio between body weight and $(height)^2$.

were found for another LTB_4 synthesis inhibitor (7), where the drug was administered and the LTB_4 response was measured during 9.5 days; desensitization or tolerance were not observed.

In a second phase I study, in which AM-24 was given in a multiple-dosing regimen, the drug showed an unexpected increase in the AUC (data on file from Industrial Farmacéutica Catabria, S.A., Spain), a phenomenon that might compromise the drug development process. The main objective of the current study was, therefore, to explore the possibility of achieving a practical dosing regimen for AM-24 by means of computer simulations. To achieve this goal, a model describing the data from the multiple-dosing study is first required. This model should then be combined with the pharmacodynamic model already established from the first phase I study data to confirm that the target concentration can be reached.

METHODS

Subjects

Thirty-two volunteers participated in this study. All participants gave their written informed consent after being given a full explanation of the trial protocol prior to their enrolment. Approval was obtained from the ethics committee of the Hospital de la Santa Creu i Sant Pau and the Spanish Drug Regulatory Agency. The study was conducted in accordance with the Declaration of Helsinki and Tokyo as well as with Good Clinical Practice. Healthy male volunteers aged between 18 and 45 years and with a body mass index within the normal range [19–26, calculated as the ratio between body weight and $(height)^2$] were admitted to the study. Table I lists the subjects' characteristics.

Volunteers were not eligible for the study if medical examination or laboratory tests were not included in the range of values established by the hospital as normal clinical values, or in cases of known gastrointestinal, hepatic, renal, respiratory, cardiovascular, metabolic, immunological, hormonal, central nervous system, or psychiatric disorders. Volunteers with chronic or relevant acute infections and history of allergy/hypersensitivity to drugs including NSAIDS, who smoked more than 10 cigarettes per day, consumed more than 45 g of alcohol per day, or were drug dependent were excluded. Intake of any other drug in the 2 weeks prior to the study was not allowed. Lastly, volunteers who had undergone surgery in the last 6 months or those who had participated in another study with an investigation drug within the 2 months preceding the study were also excluded.

Study Design

This was a randomized, double-blind, placebo-controlled, parallel single- and multiple-dose phase I study. The goal was to evaluate the pharmacokinetics and tolerability of three different oral doses of AM-24. After a 1-day screening phase performed within the 4 weeks prior to the study, the volunteers were randomized into four groups of eight subjects each, and received 240, 350, or 500 mg of AM-24 or placebo orally with 125 mL of water after a 10-h fast. Each volunteer received seven doses: A single dose was given on day 1, then AM-24 or placebo was administered once daily from day 8 to day 13. Fig. 1 shows the dosing and sampling schemes used in the current study. Volunteers arrived at the Pharmacology Research Unit at 7 a.m. on days 1 and 13 and remained there for 24 h. The participants were served standard meals for breakfast, lunch, and dinner. From days 2 to 12, volunteers arrived at 7 a.m. and left the clinic after a predose blood sampling (days 2 to 12) and intake of the next dose (days 8 to 12).

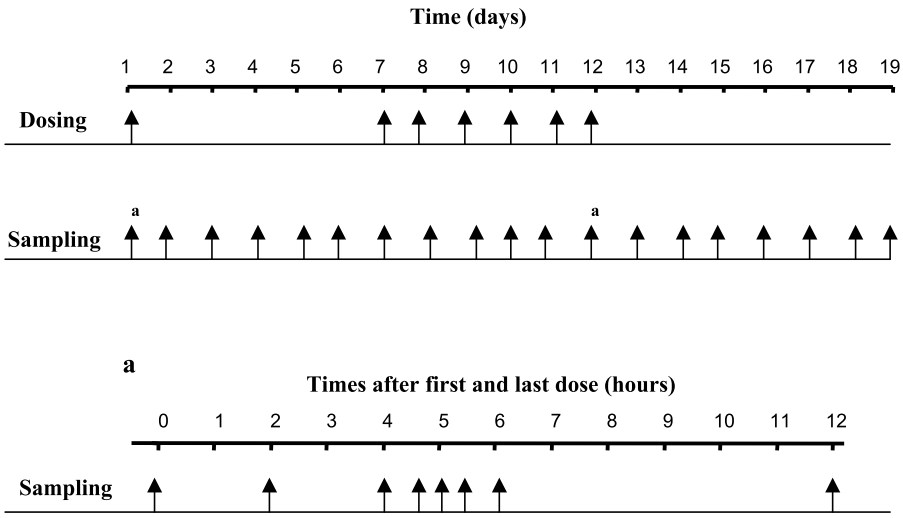

Fig. 1. Schematic representation of the dosing and blood sampling schemes used in the current study. [a], Sampling times corresponding to the days when the first and last doses were administered (the rest of the samples were taken every 24 h).

Sample Collection and Analytical Determination

Blood samples (3 mL) were taken from a heparinized catheter implanted in a forearm vein at the following times: (i) predose 2, 4, 4.5, 5, 5.5, 6, 12, 24, 48, 72, 96, 120, and 144 h after the single oral administration; (ii) predose at days 8 to 12; and (iii) predose 2, 4, 4.5, 5, 5.5, 6, 12, 24, 48, 72, 96, 120, and 144 after the last administered dose (day 13). These samples were collected in heparinized tubes and centrifuged ($1000 \times g$) at room temperature for 15 min. Plasma was then stored at $-40°C$ until analysis.

Concentrations of AM-24 in plasma were analyzed by high-performance liquid chromatography (HPLC) (8). The chromatographic system consisted of two pumps (model 510, Waters, Milford, MA, USA), an autosampler (Ultrawisp 715, Waters), a UV detector (model 486, Waters), and a system for acquisition and integration of data (Maxima 820 Chromatography Data station, Waters). Analytical separation was performed by a Nova-Pack C_{18} column (150×3.9 mm I.D., 4 μm particle size; Tecknocroma, Barcelona, Spain) at room temperature. The mobile phase, consisting of acetonitrile/water (62:38 v/v), was filtered through a 0.45-μm membrane filter (Millipore, Billerica, MA, USA) and degassed by vacuum filtering. Detection was achieved at 277 nm with a flow rate of 1 mL/min. A plasma sample (100 μL) was mixed with a volume of 100 μL of internal standard (2,6-diiodo-4-methylphenol) dissolved in acetonitrile (10 μg/mL). After addition of 1 mL of ethyl acetate, the mixture was vortexed for 3 min and centrifuged at $1000 \times g$ for 10 min. The organic phase was removed and dried under nitrogen. Residues were reconstituted in 50 μL of mobile phase and 10 μL was injected into the HPLC system. AM-24 and internal standard showed absolute recoveries of >90%. The method was linear up to 200 μg/mL. The limit of quantification was 0.1 μg/mL, and the intra- and interday coefficients of variation of the method were <12%.

Data Analysis

All pharmacokinetic data were analyzed simultaneously under the nonlinear mixed-effects modeling approach using the first-order conditional estimation method with the INTERACTION option implemented in the software NONMEM, version V (9).

Disposition characteristics of AM-24 in the body were determined by fitting mono- and multi- (two- or three-) compartment models to the data. To describe drug input, models assuming either a first- or zero-order rate of absorption, or a mixture of the two, were tested. The presence of a lag time in the absorption process was also investigated.

A preliminary exploratory analysis was done by simulating the mean pharmacokinetic profiles after multiple 240-, 350-, and 500-mg dose regimens based on the pharmacokinetic model and the mean of each of the model parameter estimates obtained from the first phase I study [the mean of each of the model parameters was calculated from the dose groups showing linear kinetics (6 to 700 mg)]. In that study data from each volunteer were analyzed individually without using the population approach. The mean values of apparent volume of the central compartment (V), total plasma clearance (CL), and first-order rate of absorption (K_A) used in the preliminary simulation were 21.4 L, 0.6 L h^{-1}, and 0.53 h^{-1}, respectively. Figure 2 shows the results from this simulation. It is clear that the previously established model behaved reasonably well after the administration of a single dose; however, observations were clearly underpredicted during

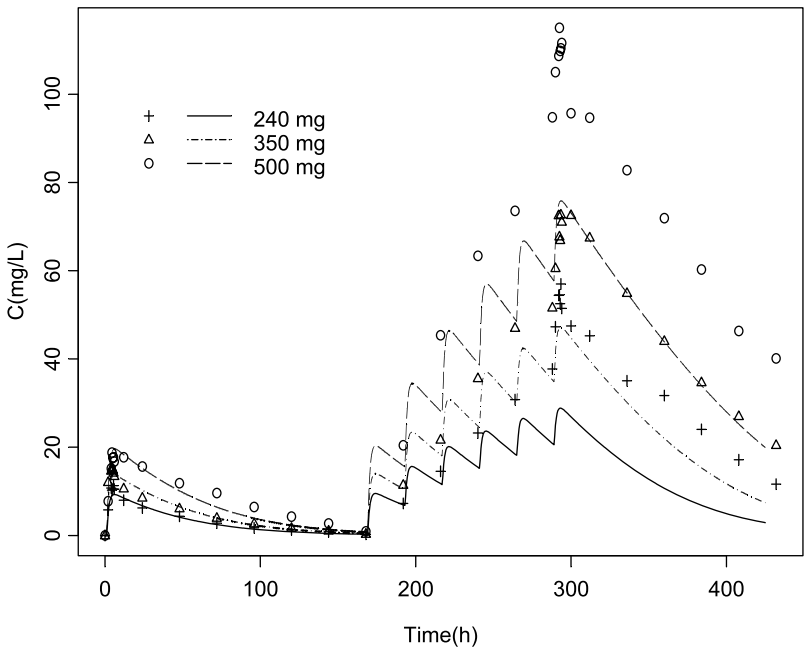

Fig. 2. Symbols represent the mean observed concentration *vs.* time profiles for each dose group. Lines correspond to the typical model predictions obtained from the selected model and mean of the model estimates obtained from the data corresponding to the first phase I clinical trial in which AM-24 was given in a single-dose regimen.

the multiple-dose treatment. Two parameters can influence AUC: bioavailability (F) and CL; in addition, CL affects the half-life of the drug. Both of them can also be modified by a change in the intrinsic enzymatic activity (CL_{INT}), among other factors.

Considering the well-stirred model for hepatic elimination (10), Eqs. (1) and (2) represent the model that has been used to relate hepatic plasma clearance (CL_H) and relative F with CL_{INT}:

$$CL_H = \frac{Q \times CL_{INT} \times f_u}{Q + CL_{INT} \times f_u} \quad (1)$$

$$F = \frac{Q}{Q + CL_{INT} \times f_u} \quad (2)$$

where Q and f_u represent the liver plasma flow and the unbound fraction in plasma, respectively. During the analysis, Q was a parameter estimated by the model, and strictly speaking, CL_{INT} represents the product between the intrinsic enzymatic activity and f_u ($CL_{INT} \times f_u$). Data from *in vitro* preclinical studies showed that f_u was low and remained constant up to AM-24 plasma concentrations of 250 mg/L (data on file from Industrial Farmacéutica Catabria, S.A., Spain).

The following models were explored to deal with the drug-induced decrease in CL_{INT}:

Model I

Michaelis-Menten kinetics (11).

$$CL_{INT} = \frac{V_{MAX}}{K_M + C} \quad (3)$$

where V_{MAX} is the maximum rate of elimination and K_M is the plasma concentration of AM-24 (C) corresponding to half of V_{MAX}.

Model II

Competitive metabolite. This model assumes the production of a hypothetical metabolite that competes with AM-24 for the binding to the enzyme responsible for its elimination:

$$CL_{INT} = \frac{\theta_{CLINT}}{1 + (C_{ME}/IC_{50M})} \quad (4)$$

$$\frac{dC_{ME}}{dt} = K_{ME}(C - C_{ME}) \quad (5)$$

where θ_{CLINT} is the value of CL_{INT} in the absence of AM-24, C_{ME} is the plasma concentration of the metabolite, IC_{50M} is a parameter scaling the inhibitory effect of C_{ME}, and K_{ME} is the first-order rate that controls the formation of C_{ME} from C. This model has been adapted from the previously published one to account for the development of tolerance to nicotine effects (12).

In the following models (Models III to V), CL_{INT} was modeled as $\theta_{CLINT} \times ENZ$, where ENZ represents the amount of enzyme. The time course of ENZ is given by:

$$\frac{dENZ}{dt} = K_{ENZ} - K_{ENZ} \times ENZ \quad (6)$$

where $dENZ/dt$ is the rate of change of ENZ and K_{ENZ} represents the rate of turnover (13). At time $t = 0$ (i.e., before administration of AM-24), $ENZ = 1$. Models III to V deal with a temporal decrease in ENZ as follows:

Model III

Reversible inhibition of the formation rate:

$$\frac{dENZ}{dt} = K_{ENZ}\left[1 - I_{MAX} \times \frac{C}{C + IC_{50}}\right] - K_{ENZ} \times ENZ \quad (7)$$

where I_{MAX} is the maximum K_{ENZ} inhibition that AM-24 can produce, and IC_{50} is the plasma concentration of AM-24 eliciting half of I_{MAX} inhibition.

Model IV

Reversible stimulation of the degradation rate:

$$\frac{dENZ}{dt} = K_{ENZ} - K_{ENZ} \times [1 + SLOPE \times C] \times ENZ \quad (8)$$

where SLOPE is a parameter governing the linear and positive relationship between K_{ENZ} *vs.* C.

Model V

Irreversible loss of enzyme amount:

$$\frac{dENZ}{dt} = K_{ENZ} - K_{ENZ} \times ENZ - K_{IRR} \times C \times ENZ \quad (9)$$

where K_{IRR} is a parameter characterizing the irreversible loss of enzymatic activity induced by AM-24.

Models I–V were also tested with simpler versions of Eqs. (1) and (2) corresponding to a drug exhibiting restrictive clearance ($CL_H = CL_{INT} \times f_u$ and $F = 1$), and to a drug exhibiting nonrestrictive clearance ($CL_H = Q$, and $F = Q/CL_{INT} \times f_u$). In addition, models where CL was the sum of CL_H and CL_2 (additional elimination pathway not being affected by administration of AM-24) were also tested.

Interindividual variability was modeled exponentially, and residual variability (reflecting the difference between the observed and model-predicted concentrations) was modeled initially with a combined error model; if one of the components (additive or proportional) of the residual error was negligible, it was deleted from the model.

Once a model providing an adequate description of the data without the incorporation of covariates was selected, patient characteristics listed in Table I were explored for significance using the generalized additive model (GAM) approach implemented in the software Xpose, version 3 (14,15). The covariates initially selected during the GAM analysis are further tested for significance in NONMEM

Table II. Results of AIC from Different Models Fitted to the Data

	Description	No. of parameters[a]	AIC
Model 0	Linear pharmacokinetics	3	5614.3
Model I	Michaelis-Menten kinetics	5	3226.9
Model II	Competitive metabolite interaction	6	3029.3
Model III	Reversible inhibition of enzyme formation	7	3002.4
Model IV	Reversible stimulation of enzyme degradation	6	3014.9
Model V	Irreversible loss of enzyme	6	3014.9

AIC, Akaike information criteria.
[a] Number corresponding to the fixed-effect parameters; the number of random-effect parameters was seven in all but model 0 ($n = 5$).

using the forward inclusion and backward elimination approach.

Selection between models was based on the precision of parameter estimates, goodness-of-fit plots, and the minimum value of objective function, −2 log(likelihood) (−2LL), provided by NONMEM. A model is declared superior to the other nested model when −2LL is reduced by 3.84 points ($p < 0.05$). Because some of the models compared were not nested, −2LL was not used directly for comparative purposes, and the value of the Akaike information criteria (AIC) (16), computed as $-2LL + 2N_p$, where N_p is the number of the parameters in the model, was used instead. The model with the lowest value of AIC, given that precision of model parameters and data description was adequate, was selected.

Pharmacokinetic model parameters were expressed as the corresponding estimate with the relative standard error (RSE). RSE was computed as the ratio between the standard error provided by NONMEM and the parameter estimate. The degree of interindividual and residual variability was expressed as coefficient of variation (%).

The final population pharmacokinetic model was explored by means of computer simulations. One thousand individual concentration *vs*. time profiles were generated for each dose group, using the fixed and random population estimates obtained from the final model. The intervals including 90% of the simulated concentrations and the profile corresponding to the median were constructed and plotted together with the raw data. The agreement between simulations and observations was judged visually.

Pharmacokinetic/Pharmacodynamic Simulations

Simulations were based on typical model parameter estimates. Table III lists the model estimates corresponding to the pharmacokinetic part of the model. In respect to pharmacodynamics, values of 100% for maximal LTB_4 synthesis inhibition and 16.6 μg/mL for IC_{50} were used. At baseline, the degree of synthesis inhibition was considered to be zero. The goal of the simulation exercise was to determine whether a steady-state plasma concentration of AM-24 can be reached and whether an appropriate percentage of LTB_4 synthesis inhibition can also be achieved shortly after the start of a long-term treatment. Different scenarios using doses of 120, 240, 350, and 500 mg of AM-24, and dosing intervals of 24 h were explored.

RESULTS

Drug absorption was well described with a first-order rate of absorption model, and there was no need to incorporate a lag time into the model ($p > 0.05$). AM-24 showed one-compartment disposition kinetics. For all the tested models, the addition of an extra elimination pathway constant over time, represented by CL_2, was significant ($p < 0.001$). Inclusion of interindividual variability was significant ($p < 0.001$) in all the pharmacokinetic parameters, with the exception of K_{ENZ} and I_{MAX}. Residual variability in the data supported the two components of the combined error model. None of the demographic characteristics listed in Table I showed significant covariate effects ($p > 0.05$).

Model for CL_H and F

When AM-24 was considered to have a nonrestrictive clearance, the models did not converge and model estimates could not be obtained. Under the AIC criteria, the assumption of a restricted elimination for AM-24 performed worse than the models using the expressions represented by Eqs. (1) and (2). However, in the latter cases, the estimates of interindividual variability for φ exceeded 150–200%. Considering the homogeneity of the population studied, this result probably indicates a model misspecification. When the typical relative bioavailability was computed using Eq. (2), its value was always >0.8. Therefore, CL_H was described as $CL_{INT} \times f_u$ and relative F was considered equal to 1, as in the case of a restricted cleared drug. Data obtained after an intravenous administration would have been very useful in the current situation to fully explore the mechanisms of the nonlinear kinetics.

Table III. Population Pharmacokinetic Model Parameter Estimates (Model III)

Parameter	Estimate	IIV
V (L)	16.2 (0.03)	12 (0.48)
θ_{CLINT} (L h^{-1})	1.23 (0.18)	35 (0.37)
CL_2 (L h^{-1})	0.103 (0.34)	30 (0.52)
K_A (h^{-1})	0.35 (0.11)	54 (0.31)
K_{ENZ} (h^{-1})	0.081 (0.14)	NE
I_{MAX}	0.98 (0.014)	NE
IC_{50} (mg L^{-1})	0.56 (0.29)	65 (0.58)
Additive residual error (mg L^{-1})	0.19 (0.19)	NA
Proportional residual error (%)	17 (0.075)	NA

Parameters are shown as estimates together with the relative standard error in parenthesis. Estimates of interindividual variability (IIV) are expressed as coefficient of variation (%).
V, apparent volume of distribution; θ_{CLINT}, plasma clearance susceptible to inhibition by the drug; CL_2, plasma clearance representing elimination routes not affected by AM-24; K_A, first-order rate constant of absorption; K_{ENZ}, rate constant governing the turnover rate of the amount of enzyme; I_{MAX}, maximum fractional decrease that AM-24 can exert on K_{ENZ}; IC_{50}, concentration of AM-24 in plasma eliciting half I_{MAX}; NE, not estimated in the model; NA, not applicable.

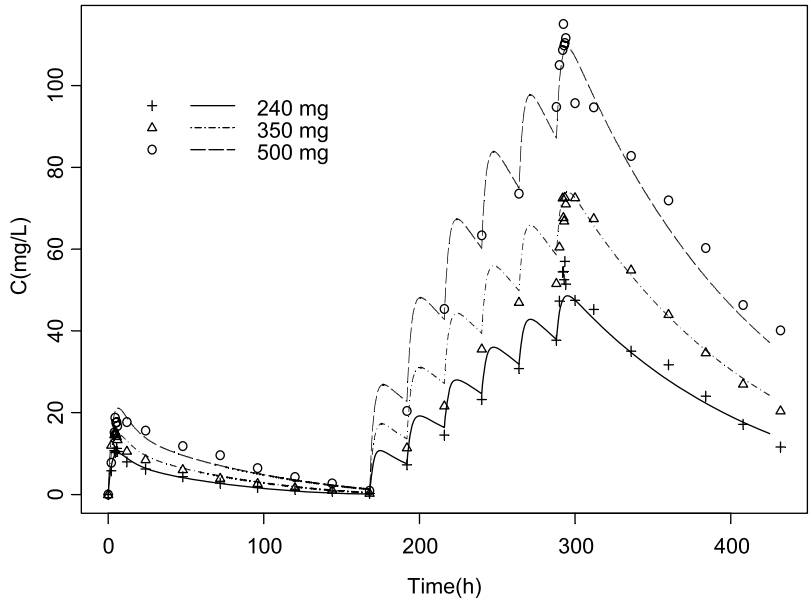

Fig. 3. Symbols represent the mean observed concentration *vs.* time profiles for each dose group. Lines correspond to the typical model predictions obtained from the model selected.

Model for CL_{INT}

Table II lists the AIC values for models I–V, including a model assuming linear kinetics, model 0 (in their full version, i.e., with all the significant random effects incorporated), obtained considering AM-24 as a restricted cleared drug. Model 0 obviously performed the worst. The models using a Michaelis-Menten kinetics (model I) or the production of a competitive metabolite (model II) behaved worse than the models including the formation and degradation of an enzyme responsible for part of the elimination of AM-24. From among latter models, model III, representing a

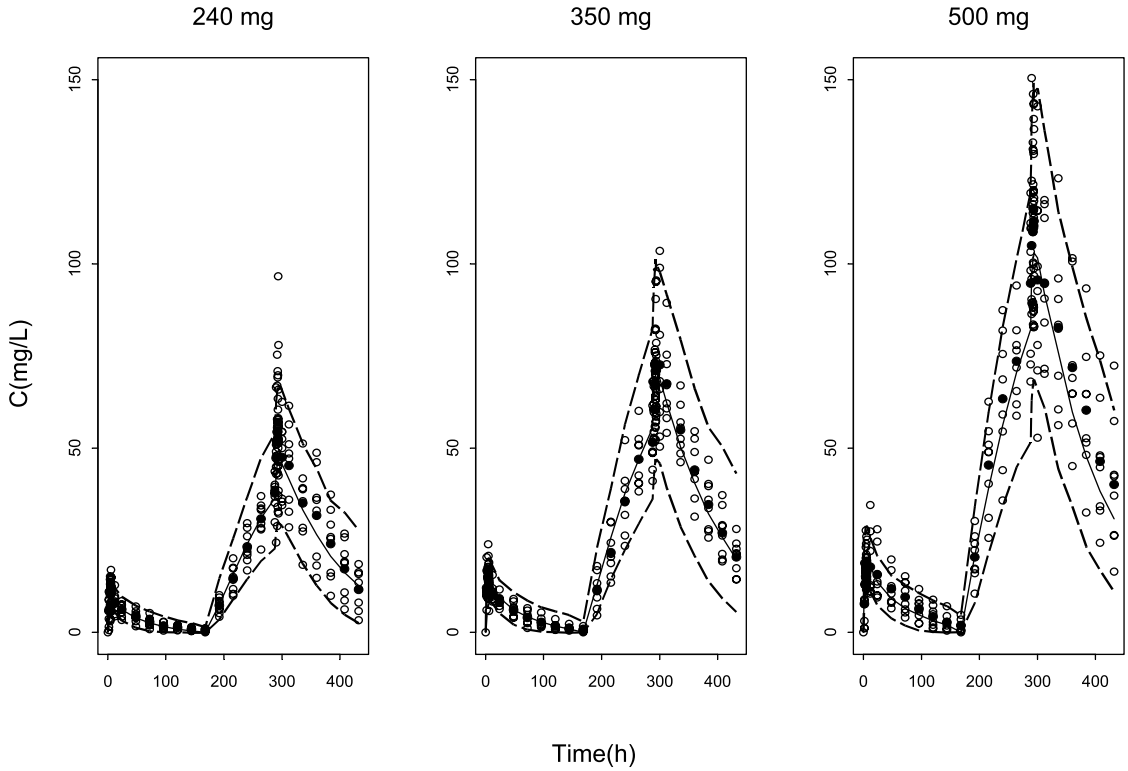

Fig. 4. Results from simulations in which 1000 virtual individuals were simulated for each dose group using the selected model and its model estimates. Dashed lines cover the area including 90% of the simulated concentrations, and solid lines represent the median of the simulated profiles. Open circles are observations, and solid circles are mean values.

reversible AM-24-induced inhibition of enzyme formation, was finally selected. Table III lists the estimates of the model parameters. All of them showed adequate precision, taking into consideration that for the random effect parameters values of RSE around 0.5 are considered acceptable.

Estimates of interindividual variability of the disposition pharmacokinetic parameters V, θ_{CLINT}, and CL_2 are low, ranging from to 12 to 35%. The variability associated to K_A and IC_{50} was 54 and 65%, respectively. The fact that interindividual variability estimates could not be obtained for K_{ENZ} and I_{MAX} might be interpreted as an identifiability issue. With regard to the response data obtained in the previous study, a population analysis was not performed, and therefore we cannot confirm if the variability found in pharmacokinetics is lower, similar, or higher than in pharmacodynamics. However, because drug plasma concentration values could be related directly with the elicited response, we expect a bigger impact of the pharmacokinetic variability on the response than in the cases where a delay between the drug in plasma and the onset of the response is present.

Figure 3 shows that the model selected was able to describe simultaneously the mean pharmacokinetic profile of each dose group adequately. Individual profiles were also well described (results not shown). In Fig. 4, the medians of the simulated profiles describe very well the median observed profiles. It is possible that the interindividual variability is slightly overestimated because the majority of the observations are located within the intervals covering 90% of the simulated values.

AM-24 was able to almost completely inhibit (98%) its main route of metabolism. The additional pathway of elimination represents less than 10% of total plasma clearance. Figure 5 shows in detail how the model behaves. After a single oral administration of 240 and 500 mg, the maximum plasma concentrations (C_{MAX}) of AM-24 were 10 and 22 mg/L, respectively (Fig. 5, left). The middle panel shows that concentrations in plasma of 2.5 and 10 mg/L are sufficient to achieve 75 and 90% inhibition of the formation rate, respectively. The estimate of 0.081 h^{-1} obtained in the selected model, which corresponds to a turnover half-life of 8.5 h, explains the fact that whereas the time to C_{MAX} is 6.5 h after administration, the time to maximal decrease in *ENZ* is approximately 2 days later (Fig. 5, right). Figure 5 also shows that the autoinhibition already occurs after single administration.

Figure 6 shows the plasma concentration *vs.* time profiles of AM-24 after administration of a 120-, 240-, 350-, and 500-mg oral dose of AM-24 once daily for a period of 28 days. Plasma drug concentrations at steady state are achieved after 3 weeks of treatment. Figure 6 shows as horizontal lines the values of plasma concentrations of AM-24 required to obtain

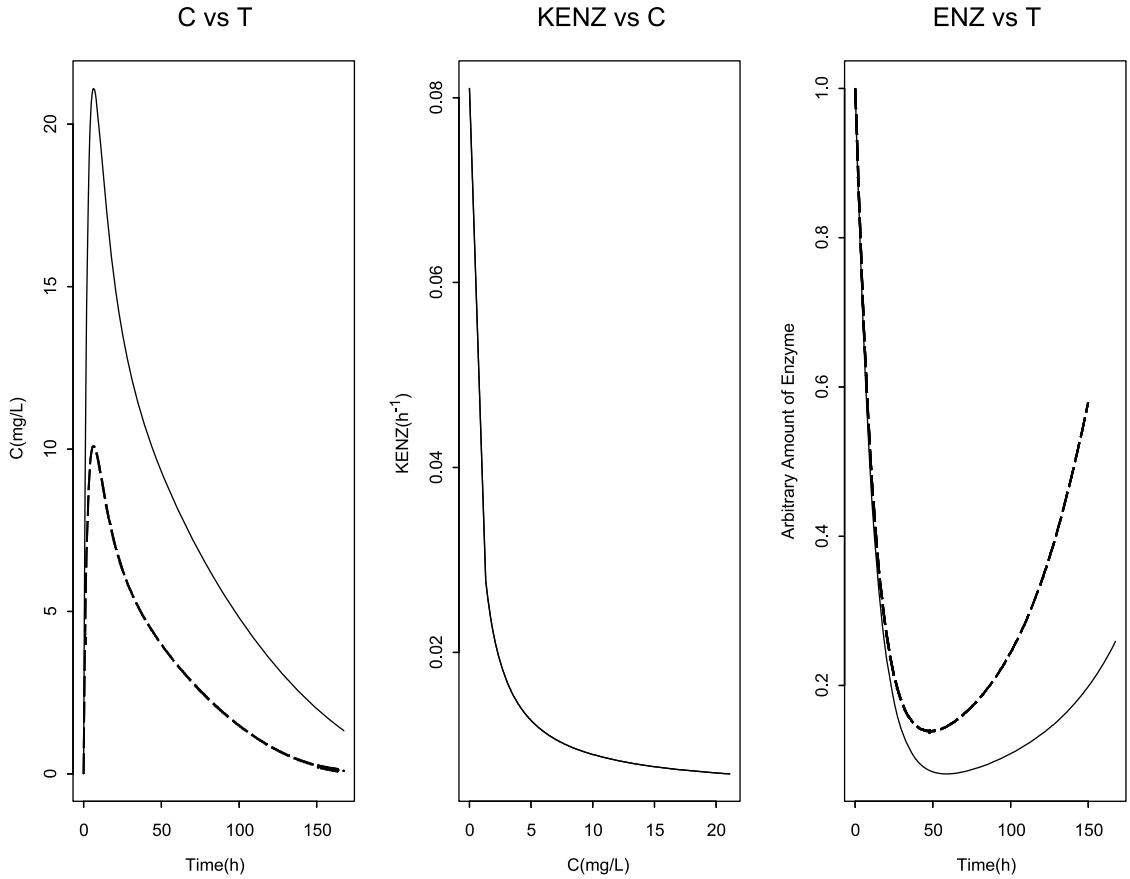

Fig. 5. Graphic details of the selected model. Left, typical model-predicted plasma concentration *vs.* time profiles after a single oral administration of AM-24 at doses of 240 mg (dashed line) and 500 mg (solid line). Middle, model-predicted relationship between rate of turnover (K_{ENZ}) and plasma concentrations (C) of AM-24. Right, time course of the arbitrary amount of enzyme (*ENZ*) after a single oral administration of AM-24 at doses of 240 (dashed line) and 500 mg (solid line).

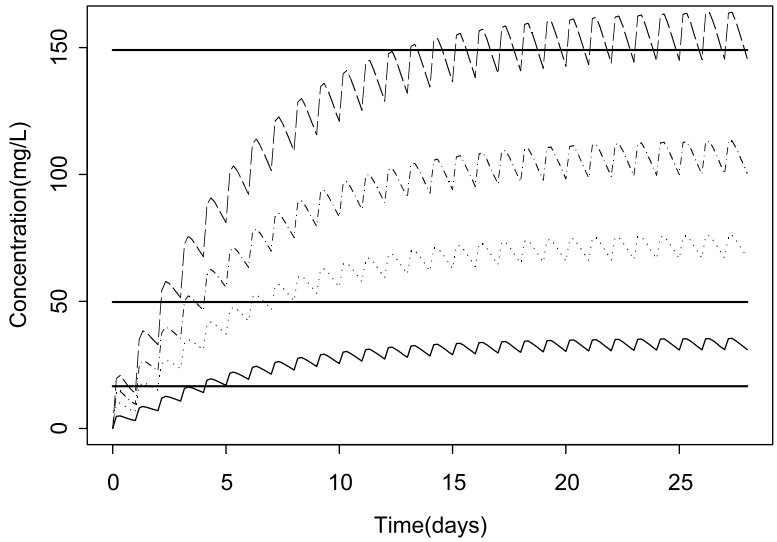

Fig. 6. Simulated plasma concentration *vs*. time profiles of AM-24 after 28 days of once-daily oral administration at doses of 120, 240, 350, and 500 mg. Solid horizontal lines show the plasma levels of AM-24 required to achieve a 50, 75, or 90% maximal LTB_4 synthesis inhibition.

50% (16.6 mg/L), 75% (49.8 mg/L), and 90% (149 mg/L) of LTB_4 synthesis inhibition. Dosing regimens consisting of 240, 350, or 500 mg given once daily produce at steady-state percentages of LTB_4 synthesis inhibition higher than 75%. If maximal inhibition is needed, the maintenance dose should be 500 mg. Simulations suggest that the use of loading dose might be not necessary because a 75% of maximal LTB_4 synthesis inhibition is achieved in the third day of treatment for the dosing regimens based on the highest doses—350 and 500 mg. The 500-mg dose is a safe and well-tolerated dose with respect to adverse events, although two, three, and two volunteers in the 240-, 350-, and 500-mg dose groups, respectively, experienced a mild transient nonclinically relevant hypothyroidism.

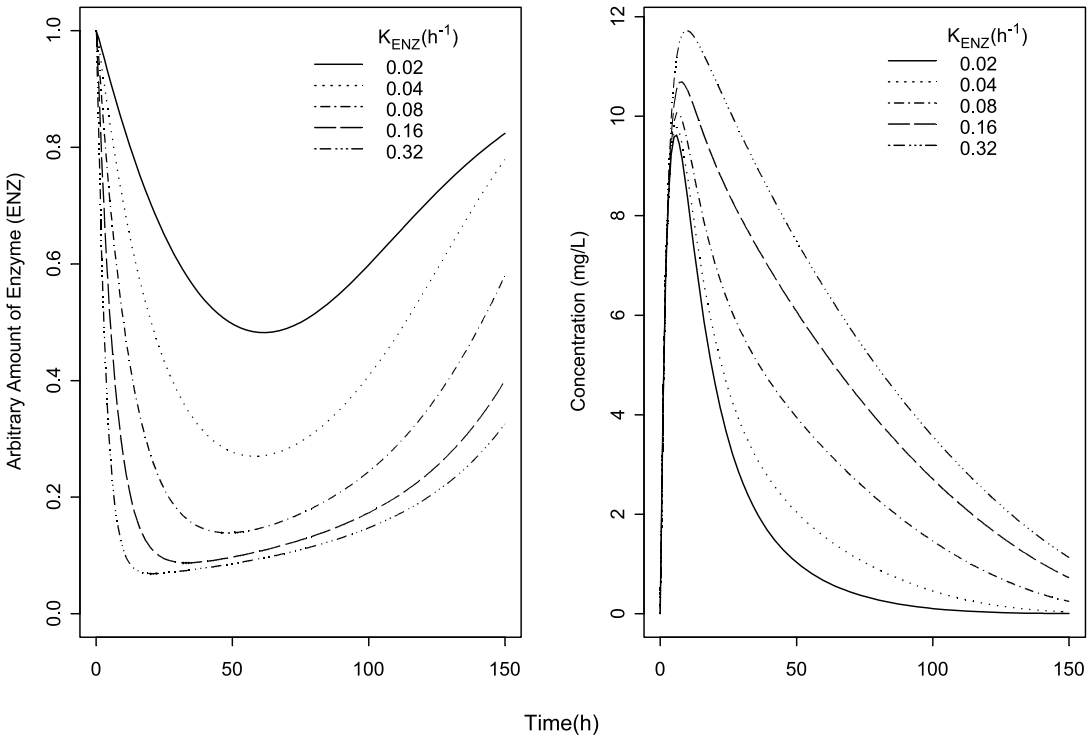

Fig. 7. Role of the magnitude of the rate of turnover, K_{ENZ}, on the time profiles of the arbitrary amount of enzyme, *ENZ* (left), and plasma concentrations of AM-24 (right). Simulations were performed assuming a single 240-mg oral dose of AM-24.

DISCUSSION

The presence of a certain complexity in the pharmacokinetics of a new drug does not necessarily represent a reason to discontinue its development. Tolerance development and delayed onset of action with respect to the plasma drug kinetics are examples of complexities in the response that can be understood and predicted with the use of appropriate models (17,18).

In the current study, a drug in early clinical development showed clear nonlinear pharmacokinetics after multiple oral dosing. In this situation, it is therefore important to know if a steady state can be achieved after multiple dose administration, in other words, whether or not plasma clearance can be completely inhibited. If a steady state can be reached, the possibility to design a practical dosing regimen to obtain the therapeutic goals has then to be explored.

To address the first point, data modeling is required. The selected model will help to identify whether the nonlinearity is due to an increase in bioavailability, a decrease in total plasma clearance, or both, and if there is more than one elimination pathway.

Nonlinear elimination has been modeled in the past using Michaelis-Menten saturation kinetics (11); other authors have used circadian variations, as in the case of nicotine (19) or more frequently assuming that elimination is a function of an enzyme. The levels of this enzyme are maintained in baseline conditions by the balance between synthesis and degradation, processes that can be modified by plasma drug concentrations in this type of model (13,20). More elaborate models including the active and inactive status of the enzyme have also been proposed (21,22). Such models are far from being fully mechanistic, but they are useful to explore different dosing scenarios as they use plasma or metabolite concentrations as the driving force to cause time-dependent alterations of the enzyme amount. Other more empirical models where the time from the start of the treatment is used as the predictor variable have been also proposed (23). As we do not know the exact mechanism responsible for the increase in AUC, several models were tested. If the drug is given intravenously, changes in AUC reflect a change in total plasma clearance. However, if the drug is given orally, as in the case of the current evaluation, a change in AUC can be the consequence of a change in CL and F. Assuming a well-stirred model for drug elimination, in the case of a nonrestricted cleared drug, CL would be independent of CL_{INT} and F would be inversely related to CL_{INT}. If elimination is restricted, CL is proportional to changes in CL_{INT}, and F has a value close to 1. Because information about the absolute bioavailability was not available, models considering a restricted, intermediate [represented by Eqs. (1) and (2)], and nonrestricted clearance were fitted to the data. On the basis of the model selection criteria, CL seemed to be the parameter showing the nonlinearity.

Unfortunately, due to the data generated at the time, which did not include information after intravenous administration, it was not possible to further explain the mechanisms of enzyme inhibition and the enzymes involved. There are examples in the literature showing that several enzymes responsible for drug elimination become (auto)inhibited after continuous exposure. High levels of 3′-azido-3′-deoxythymidine (AZT) in cultured primary placental cells induced a decrease in uridine diphosphate glucuronosyltransferase, resulting in an autoinhibition of AZT metabolism (24). CYP 2D6 activity was found to be decreased after 6 weeks of continuous paroxetine administration (25), and the long-acting calcium antagonist mibrefadil inhibits its own metabolism, decreasing the CYP 3A4 activity (26). In none of these studies was an attempt to model the kinetics of the autoinhibition undertaken, and therefore a comparison across model parameter estimates is not possible because, to our knowledge, the current study is the first to report a modeling of clearance autoinhibition. However, models dealing with enzyme induction have reported estimates for the K_{ENZ} (h^{-1}) parameter [0.027 (20), 0.041 (21), 0.034 (22)] that are of the same order as that reported in the present study (0.081). The effect of the magnitude of the parameter K_{ENZ} on the plasma concentration *vs*. time profiles of AM-24 is shown in the right panel of Fig. 7 for a single 240-mg oral dose of AM-24. It can be observed that K_{ENZ} has a clear impact on the pharmacokinetics of the drug. The left panel in Fig. 7 shows the kinetics of the arbitrary amount of enzyme, where the fastest onset and offset of the autoinhibitory effects correspond to the highest values of K_{ENZ}.

As another noninhibited elimination pathway was supported by the data and as the estimate of I_{MAX} was significantly different from 1 ($p < 0.001$), we were able to anticipate that a steady state could be reached. However, computer simulations were needed to investigate when the appropriate target plasma concentration would be achieved after treatment was started. Diseases that require LTB_4 inhibition, such as asthma, psoriasis, rheumatoid arthritis, and inflammatory bowel disease (27), are long-duration diseases and, therefore, it is not of maximum importance to achieve the target plasma concentration immediately after the beginning of the treatment. In the case of AM-24, simulations have shown that (i) steady-state conditions can be reached after 3 weeks of treatment, (ii) 90% of maximal LTB_4 synthesis inhibition can be achieved at steady-state by administering 500 mg once daily, and (iii) 75% of maximal LTB_4 synthesis inhibition can be achieved at the third day of treatment by using the same dosing regimen. With respect to adverse events, single doses of up to 1200 mg and multiple-dose administration of 500 mg were exempt from moderate and serious adverse events and showed excellent tolerability.

In conclusion, an extensive modeling exercise was undertaken to describe the nonlinearity observed after a multiple, once-daily administration of AM-24, a compound that showed linear kinetics after a single administration. AM-24 was able to inhibit its main route of metabolism—although not completely—and a second minor pathway of elimination was found. These two results ensure that a steady state can be achieved, and simulations have shown that steady-state conditions eliciting 90% of maximal LTB_4 synthesis inhibition can be reached after 3 weeks during oral treatment with AM-24 administered at the dose of 500 mg once daily.

ACKNOWLEDGMENTS

We would like to thank Antoni Mollins for his help in the analytical determination of AM-24 plasma concentra-

tions. Marta Valle was supported by a grant from the Spanish Healthy Department (CP 04/00121) in collaboration with the Institut de Recerca de l'Hospital de la Santa Creu i Sant Pau. This work was partially supported by a grant from Industrial Farmacéutica Catabria, S.A., Spain.

REFERENCES

1. R. A. Prentis, Y. Lis, and S. R. Walker. Pharmaceutical innovation by the seven UK-owned pharmaceutical companies (1964–1985). *Br. J. Clin. Pharmacol.* **25**:387–396 (1988).
2. D. K. Walker. The use of pharmacokinetic and pharmacodynamic data in the assessment of drug safety in early drug development. *Br. J. Clin. Pharmacol.* **58**:601–608 (2004).
3. B. Y. Kim, J. H. Jeong, K. Park, and J. D. Kim. Bioadhesive interaction and hypoglycemic effect of insulin-loaded lectin–microparticle conjugates in oral insulin delivery system. *J. Control. Release* **102**:525–538 (2005).
4. I. Echevarria, C. Barturen, M. J. Renedo, I. F. Troconiz, and M. C. Dios-Vieitez. Comparative pharmacokinetics, tissue distributions, and effects on renal function of novel polymeric formulations of amphotericin B and amphotericin B-deoxycholate in rats. *Antimicrob. Agents Chemother.* **44**:898–904 (2000).
5. L. Aarons, M. O. Karlsson, F. Mentré, F. Rombout, J. L. Steimer, and A. van Peer and invited COST B15 experts. Role of modelling and simulation in Phase I development. *Eur. J. Pharm. Sci.* **13**:115–122 (2001).
6. P. Olsson Gisleskog, D. Hermann, M. Hammarlund-Udenaes, and M. O. Karlsson. The pharmacokinetic modelling of GII98745 (dutasteride) a compound with parallel linear and nonlinear elimination. *Br. J. Clin. Pharmacol.* **47**:53–58 (1998).
7. M. Depre, B. Friedman, A. Van Hecken, I. de Lepeleire I, W. Tanaka, A. Dallob, S. Shingo, A. Porras, C. Lin, and P. J. de Schepper. Pharmacokinetics and pharmacodynamics of multiple oral doses of MK-0591, a 5-lipoxygenase-activating protein inhibitor. *Clin. Pharmacol. Ther.* **56:**22–30 (1994).
8. L. Garcia-Capdevila, C. Lopez-Calull, S. Pompermayer, C. Arroyo, A. M. Molins-Pujol, and J. Bonal. High-performance liquid chromatography analysis of Bobel-24 in biological samples for pharmacokinetic, metabolic and tissue distribution studies. *J. Chromatogr. B Biomed. Sci. Appl.* **708**:169–175 (1998).
9. S. L. Beal and L. B. Sheiner. *NONMEM Users Guides.* NONMEM Project Group, University of California at San Francisco, San Francisco, CA, 1992.
10. K. S. Pang and M. Rowland. Hepatic clearance of drugs. I. Theoretical considerations of a "well-stirred" model and a "parallel tube" model. Influence of hepatic blood flow, plasma and blood cell binding, and the hepatocellular enzymatic activity on hepatic drug clearance. *J. Pharmacokinet. Biopharm.* **5**: 625–653 (1977).
11. P. O. Gisleskog, D. Hermann, M. Hammarlund-Udenaes, and M. O. Karlsson. The pharmacokinetic modeling of GI198745 (dutasteride), a compound with parallel linear and nonlinear elimination. *Br. J. Clin. Pharmacol.* **47**:53–58 (1999).
12. H. C. Porchet, N. L. Benowitz, and L. B. Sheiner. Pharmacodynamic model of tolerance: application to nicotine. *J. Pharmacol. Exp. Ther.* **244**:231–236 (1988).
13. C. von Bahr, E. Steiner, Y. Koike, and J. Gabrielsson. Time course of enzyme induction in humans: effect of pentobarbital on nortriptyline metabolism. *Clin. Pharmacol. Ther.* **64**:18–26 (1998).
14. J. W. Mandema, D. Verotta, and L. B. Sheiner. Building population pharmacokinetic–pharmacodynamic models. I. Models for covariate effects. *J. Pharmacokinet. Biopharm.* **20**:511–528 (1992).
15. E. N. Jonsson and M. O. Karlsson. Xpose: an Splus based population pharmacokinetic/pharmacodynamic model building aid for NONMEM. *Comput. Methods Programs Biomed.* **58**:51–64 (1999).
16. T. M. Ludden, S. L. Beal, and L. B. Sheiner. Comparison of the Akaike information criterion, the Schwarz criterion and the *F* test as guides to model selection. *J. Pharmacokinet. Biopharm.* **22**:431–445 (1994).
17. M. Gardmark, L. Brynne, M. Hammarlund-Udenaes, and M. O. Karlsson. Interchangeability and predictive performance of empirical tolerance models. *Clin. Pharmacokinet.* **36**:145–167 (1999).
18. T. Kerbusch, P. A. Milligan, and M. O. Karlsson. Assessment of the relative *in vivo* potency of the hydroxylated metabolite of darifenacin in its ability to decrease salivary flow using pooled population pharmacokinetic–pharmacodynamic data. *Br. J. Clin. Pharmacol.* **57**:170–180 (2004).
19. J. M. Gries, N. Benowitz, and D. Verotta. Importance of chronopharmacokinetics in design and evaluation of transdermal drug delivery systems. *J. Pharmacol. Exp. Ther.* **285**:457–463 (1998).
20. M. Hassan, U. S. Svensson, P. Ljungman, B. Bjorkstrand, H. Olsson, M. Bielenstein, M. Abdel-Rehim, C. Nilsson, M. Johansson, and M. O. Karlsson. A mechanism-based pharmacokinetic-enzyme model for cyclophosphamide autoinduction in breast cancer patients. *Br. J. Clin. Pharmacol.* **48**:669–677 (1999).
21. A. D. Huitema, R. A. Mathot, M. M. Tibben, S. Rodenhuis, and J. H. Beijnen. A mechanism-based pharmacokinetic model for the cytochrome P450 drug–drug interaction between cyclophosphamide and thioTEPA and the autoinduction of cyclophosphamide. *J. Pharmacokinet. Pharmacodyn.* **28**:211–230 (2001).
22. M. E. de Jonge, A. D. Huitema, S. Rodenhuis, and J. H. Beijnen. Integrated population pharmacokinetic model of both cyclophosphamide and thiotepa suggesting a mutual drug–drug interaction. *J. Pharmacokinet. Pharmacodyn.* **31**:135–156 (2004).
23. P. L. Bonate, S. Floret, and C. Bentzen. Population pharmacokinetics of APOMINE: a meta-analysis in cancer patients and healthy males. *Br. J. Clin. Pharmacol.* **58**:142–155 (2004).
24. A. C. Collier, J. A. Keelan, P. E. Van Zijl, J. W. Paxton, M. D. Mitchell, and M. D. Tingle. Human placental glucuronidation and transport of 3′azido-3′-deoxythymidine and uridine diphosphate glucuronic acid. *Drug Metab. Dispos.* **32**:813–820 (2004).
25. L. K. Solai, B. G. Pollock, B. H. Mulsant, R. F. Frye, M. D. Miller, R. A. Sweet, M. Kirshner, D. Sorisio, A. Begley, and C. F. Reynolds III. Effect of nortriptyline and paroxetine on CYP2D6 activity in depressed elderly patients. *J. Clin. Psychopharmacol.* **22**:481–486 (2002).
26. H. A. Welker, H. Wiltshire, and R. Bullingham. Clinical pharmacokinetics of mibefradil. *Clin. Pharmacokinet.* **35**: 405–423 (1998).
27. W. G. Tong, X. Z. Ding, R. Henning, R. C. Witt, J. Standop, P. M. Pour, and T. E. Adrian. Leukotriene B4 receptor antagonist LY293111 inhibits proliferation and induces apoptosis in human pancreatic cancer cells. *Clin. Cancer Res.* **8**:3232–3242 (2002).